ANTICANCER RESEARCH *29*: 4949-4958 (2009)

Simultaneous Identification and Quantification of Proteins by Differential $^{16}O/^{18}O$ Labeling and UPLC-MS/MS Applied to Mouse Cerebellar Phosphoproteome Following Irradiation

DOMINIC WINTER[1], JOERG SEIDLER[1], SHELLY ZIV-LEHRMAN[2], YOSEF SHILOH[2] and WOLF D. LEHMANN[1]

[1]Molecular Structure Analysis, German Cancer Research Center, 69120 Heidelberg, Germany;
[2]Department of Human Molecular Genetics and Biochemistry,
Sackler School of Medicine, Tel Aviv University, Tel Aviv 69978, Israel

Abstract. *Differential proteolytic ^{18}O labeling is a cost-effective but not commonly used method in the field of quantitative proteomics based on mass spectrometry (MS). In most cases, peptide identification is performed at the MS/MS level followed by peptide quantification at the MS level. In this study, identification and quantification of ^{18}O-labeled peptides was performed in a single step at the MS/MS level using the MASCOT 2.2 search engine, and the instrumental conditions for acquisition of ultra performance liquid chromatography electrospray MS/MS (UPLC-ESI-MS/MS) data were adapted accordingly. Using analysis of standard peptide and protein mixtures prepared by differential $^{16}O/^{18}O$ labeling, under these conditions automated MS/MS data acquisition and evaluation delivered correct data. Linearity and reproducibility of this approach indicated excellent performance. In addition, the method was applied to relative quantification of protein phosphorylation in mouse brain following treatment with ionizing radiation. The analysis led to automated quantification of 342 proteins and 174 phosphorylation sites, 24 of which were up- or down-regulated by a factor of 2 or more. The majority of these phosphorylation sites were found to be located in target sequences of known protein kinases, showing the activation of kinase-regulated signaling cascades by irradiation.*

Enzymatic digestion of proteins in ^{18}O-enriched water is an elegant, versatile and cost-effective labeling method in analytical proteomics. It has been applied for peptide sequencing (1), *de novo* peptide sequencing (2-4), relative peptide quantification (5-7), relative quantification of subproteomes (8-12), and relative quantification of protein phosphorylation (13). Other applications of $^{16}O/^{18}O$ labelling are the recognition of glycosylation (14-16), disulfide-linked peptides (16), isoaspartate formation (17, 18), succinimide formation (19), and deamidation (20). Methods and applications of proteolytic ^{18}O labeling of peptides have been reviewed elsewhere (21, 22).

In the field of quantitative analytical proteomics, proteolytic ^{18}O labeling has experienced slower methodological development compared to other chemical or metabolic labeling methods (23-27). Putative downsides of the ^{18}O labeling method are the time required, variability of ^{18}O incorporation, the possibility of back exchange of the label, a relatively small mass shift, and the lack of suitable data evaluation software.

The time required for ^{18}O labeling is identical to that for the digestion procedure. Thus, ^{18}O labeling can be achieved in 15 to 30 min by acceleration of enzymatic digestion, *e.g.* using immobilized trypsin (28), ultrasonic radiation or elevated temperature (29).

Several attempts have been undertaken to overcome the variable label introduction of one or two atoms of ^{18}O, by either trying to achieve the incorporation of a single ^{18}O atom (30), or complete labeling by two atoms of ^{18}O (16, 31). The defined introduction of one or two ^{18}O atoms simplifies the quantitative evaluation of a mixed (labeled + unlabeled) isotopic pattern, since in this case, the isotopic pattern consists of only two components ($^{16}O/^{18}O$ or $^{16}O/^{18}O_2$). In cases of variable incorporation, the deconvolution process must consider three components (^{16}O + ^{18}O + $^{18}O_2$), where the sum of the ^{18}O and the $^{18}O_2$ isotopomer represents the amount of the labeled species. This sum is independent of the relative composition since an interconversion of the ^{18}O species into the $^{18}O_2$ species does not change the sum of both species.

Correspondence to: Professor Dr. Wolf D. Lehmann, Molecular Structure Analysis (W160), German Cancer Research Center, Im Neuenheimer Feld 280, 69120 Heidelberg, Germany. Tel: +49 6221424563, Fax: +49 6221424561, e-mail: wolf.lehmann@dkfz.de

Key Words: Phosphoproteome, UPLC, IMAC, cerebellum, oxygen-18.

Back exchange of the ^{18}O label can occur by an acid-catalyzed (at pH<2) or protease-catalyzed mechanism (32-34). In practice, ^{18}O back exchange can be avoided effectively by denaturing or removal of the protease used for digestion, *e.g.* by using immobilized trypsin (35) and by avoiding pH values <2 subsequent to the labeling step.

Several software programs for the deconvolution of molecular ion isotopic patterns of ^{18}O labeled peptides have been developed (*e.g.* (36-38)) but to our knowledge, most of these programs are currently not available as open access files or require expert software knowledge. As an alternative to the deconvolution of molecular ion patterns, the ^{18}O content of peptides can be analyzed at the fragment ion level. By concept, evaluation at the tandem mass spectrometry (MS)/MS level should provide a better accuracy of the quantitative data compared to the evaluation of survey spectra, due to reduced background and an increased specificity (39). Recently, software for quantitative evaluation of labeling experiments with ^{13}C- and ^{15}N-labeled peptides at the MS/MS level was introduced (39). A version of this software that is applicable to ^{18}O labeling was incorporated into the search engine MASCOT (version 2.2). Here, we demonstrate the performance of this software using mixtures of standard peptides/proteins. Finally, we present the first application of differential ^{18}O labeling to one-step identification and relative quantification of site-specific protein phosphorylation in a complex protein sample using this software.

Materials and Methods

Chemicals. All chemicals were from Sigma (Deisenhofen, Germany) unless indicated otherwise. Trypsin was from Roche (Mannheim, Germany). All solvents and acids were from Biosolve (Valkenswaard, the Netherlands) in ULC grade quality suitable for ultra performance liquid chromatography. ^{18}O-Enriched water (≥98% purity) was from Rotem (Leipzig, Germany).

Standard mixture preparation. Synthetic peptides were kindly produced in-house using Fmoc chemistry in the Central Peptide Synthesis Unit of the DKFZ by Dr. R. Pipkorn. Three differently $^{16}O/^{18}O$-labeled mixtures of the peptide DLESQLAQSR were prepared. Fractions of the synthetic peptide were incubated either in ^{16}O or ^{18}O water, respectively, in the presence of trypsin for 24 h. Trypsin was removed and the samples were desalted using ZipTips (Millipore, Billerica, MA, USA). Subsequently ^{16}O- and ^{18}O-labeled samples were combined and the resulting ratios of nonlabeled/labeled compounds controlled by nano electrospray (ESI)-MS revealing the ratios present in the mixtures (9:1, 1:1, 1:9). Differentially $^{16}O/^{18}O$-labeled protein digest mixtures were prepared from ovalbumin. For this purpose, 100 μg of ovalbumin were dissolved in 0.1M NH_4HCO_3, denatured using 4 M urea, reduced and alkylated using dithiothreitol (DTT) and iodoacetamide (IAA) and then digested in solution in ^{16}O and ^{18}O water, respectively, using trypsin. After digestion, the labeled and unlabeled fractions were mixed in different ratios.

Complex protein sample preparation and SCX/WAX peptide fractionation. Cerebellum tissues were prepared from untreated and irradiated (10 Gy, excised 1 h after irradiation) 10-day-old Balb-C mice. Proteins were extracted in the presence of protease and phosphatase inhibitors (both from Roche). A quantity of 3 mg protein of each fraction was precipitated using cold acetone and the precipitate was washed once using acetone. After removing the acetone, the precipitate was dried using a Speed Vac and resuspended using 0.1 M NH_4HCO_3 in ^{18}O or ^{16}O water, respectively. In the next step, in-solution digestion was carried out as described above. Resulting peptides were desalted using an XBridge BEH 130 PREP C_{18} 250 mm × 10 mm reversed-phase column with a particle diameter of 5 μm (Waters, Milford, MA, USA). The volume of the desalted peptide fractions was reduced using a Speed Vac. Peptides were then loaded onto an SCX/WAX (1:2) 200 mm × 4.4 mm column with a particle diameter of 5 μm and 300 Å pore size (PolyLC Inc., Columbia, MD, USA) and a linear gradient from 100% A (20% acetonitrile, 0.1% formic acid), 0% B (20% acetonitrile, 0.1% formic acid, 0.5 M ammonium acetate) to 0% A, 100% B in 40 min was applied. During elution, 20 fractions were collected, the volume was reduced using a Speed Vac and the samples were desalted using the preparative reversed-phase column. Desalted fractions were again reduced in volume using a Speed Vac. 5% to 50% of each fraction was submitted to phosphopeptide enrichment by Ga^{3+} immobilized metal ion affinity chromatography (IMAC) (Phosphopeptide Isolation Kit, Pierce, Rockford, IL, USA). Flow-through fractions and phosphopeptide fractions were reduced in volume and citrate was added to the phosphopeptide fractions to a final concentration of 50 mM (40).

UPLC-MS/MS analyses. All LC-MS/MS analyses were carried out using a nanoAcquity UPLC system (Waters). The column used was a 150 mm × 75 μm C_{18} BEH column packed with 1.7 μm particles with a pore size of 130 Å. Samples were loaded directly onto the analytical column without using a trap column. After sample loading followed by 24 min of washing with 1% solvent A (water with 0.1% formic acid), a linear gradient of 60 min length was applied from 99% A, 1% B (acetonitrile with 0.1% formic acid) to 70% A and 30% B. The column temperature was 35˚C and the flow was 400 nl/min. The column outlet was connected to a pico tip sprayer (Waters Micromass, Manchester, UK) using PicoTips (New Objective, Woburn, MA, USA) mounted on a Quadrupole Time-of-Flight mass spectrometer (QTOF-2, Waters Micromass, Manchester, UK). The capillary voltage applied was 2400 V. The mass spectrometer was operated in data-directed acquisition (DDA) mode with recording of 1 spectrum per second. Following one survey scan, the two most abundant signals in each scan were selected for fragmentation and up to two MS/MS scans per precursor ion were acquired. For the low and high mass resolution, a value of 2 was selected, resulting in a transmission window of 12 m/z units extending from about –3 m/z to +9 m/z relative to the selected set mass for MS/MS.

Data processing. Using MassLynx 4.1 (Waters) the MS/MS raw data were transformed into peak lists (.pkl files). For processing, no smoothing or background subtraction was applied. The individual .pkl files obtained in the analysis of the mouse brain samples were merged into a single file using the program merge.pl provided by matrixscience (www.matrixscience.com). All .pkl files were searched against the MSDB database (http://csc-fserve.hh.med.ic.ac.uk/msdb.html) using MASCOT 2.2 installed on an in-house server. As

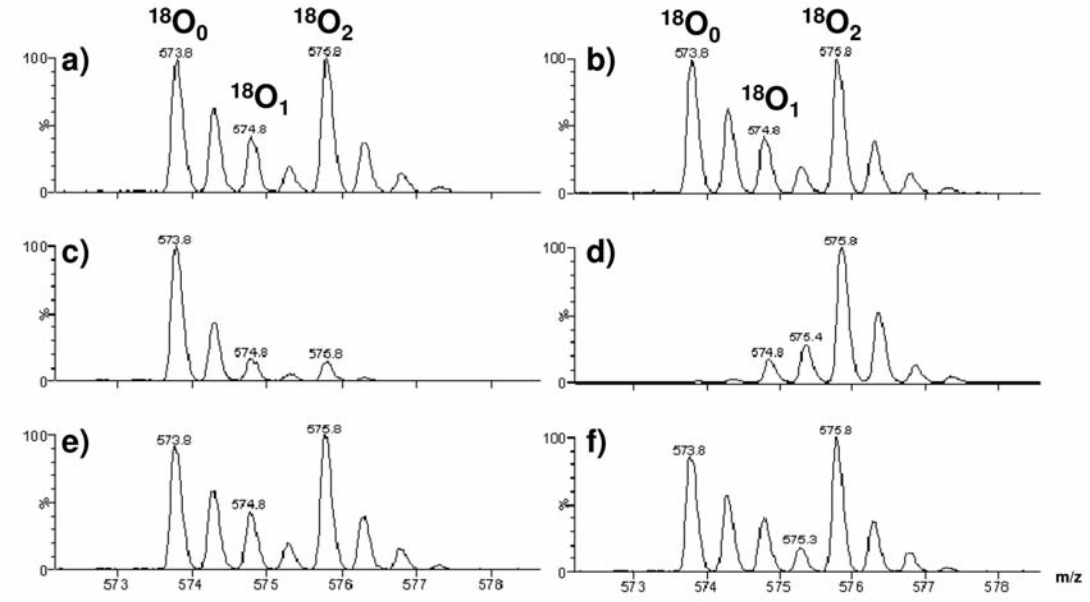

Figure 1. *Impact of the precursor ion transmission window on the isotopic pattern transmission of a 1:1 $^{16}O/^{18}O$ mixture of DLESQLAQSR ($C^{16}O^{16}OH$) and DLESQLAQSR ($C^{18}O^{18}OH$); a) and b) are identical and show the isotopic pattern of the $[M+2H]^{2+}$ ion recorded in survey mode; c) set mass m/z 573.8 using the standard window; d) set mass m/z 575.8 using the standard window; e) set mass m/z 573.8 using the extended window; f) set mass m/z 575.8 using the extended window. With the standard window, the isotopic pattern is only partly transmitted (c, d), whereas use of the extended window leads to a transmission of the complete pattern (e, f).*

search parameters, the option 'quantification by ^{18}O-corrected multiplex' was selected in combination with a precursor mass tolerance window of 6 Da and an MS/MS mass tolerance window of 0.3 Da. The instrument specification was set as ESI-QUAD-TOF. As digestion parameters, trypsin in combination with a maximum of 3 miscleavages were selected. Carbamidomethyl cysteine was selected as fixed and methionine oxidation as reversible modification. For phosphopeptide analysis, phosphorylation at serine, threonine or tyrosine was set as additional variable modification. Average values, standard deviations and correlation coefficients were calculated using Microsoft Excel.

Results

To obtain reliable and correct quantitative results, at first binary and complex peptide standard mixtures with known ratios of $^{16}O/^{18}O$ content at the C-terminus were used to optimize the LC-MS/MS settings and the search engine parameters (see Material and Methods).

$^{16}O/^{18}O$ Labeling and MS/MS spectra acquisition. For correct quantification at the MS/MS level, the broad isotopic envelopes of proteolytically ^{18}O-labeled peptides must be completely included in the precursor ion transmission window. Only under these conditions do the isotopic patterns of the y ions provide a $^{16}O/^{18}O$ ratio which is identical to that of the molecular ion. In the DDA mode, the two extreme cases that can occur are that either the most abundant peak of the nonlabeled species or that of the doubly ^{18}O-labeled species is selected as set mass for the registration of an MS/MS spectrum. Using the 1:1 mixture of DLESQLAQSR ($C^{16}O^{16}OH$) and DLESQLAQSR ($C^{18}O^{18}OH$) both situations were studied by nanoESI-MS and manual set mass selection. Figure 1a and b demonstrate that under standard conditions, this situation is not met, since the precursor ion isolation window extends from –0.5 m/z to 2.5 m/z relative to the set mass. This results in only partial transmission of the molecular ion group, as shown in Figure 1c and d. A shift of the left border of the precursor ion window to –2 m/z would result in complete transmission for both set mass alternatives (Figure 1e, f) for molecular ions of charge state 2 or higher. To meet these conditions, the width of the precursor ion transmission window was enlarged to approximately 12 m/z units. This window extends from about –3 m/z to +9 m/z relative to the set mass.

Using this extended precursor ion transmission window, the complete isotopic pattern, including the unlabeled as well as the singly and doubly labeled form of the peptide, is transmitted. The resulting MS/MS spectra show unlabeled b ions and ^{18}O-labeled y ions. As an example, the survey spectra and the MS/MS spectra showing the ^{18}O-labeled y_2 ion of 3 different mixtures of the synthetic peptides DLESQLAQSR ($C^{16}O^{16}OH$) and DLESQLAQSR ($C^{18}O^{18}OH$) are shown in Figure 2. This Figure proves that quantification can be performed on the MS/MS level, since the isotopic patterns of connected molecular ions and

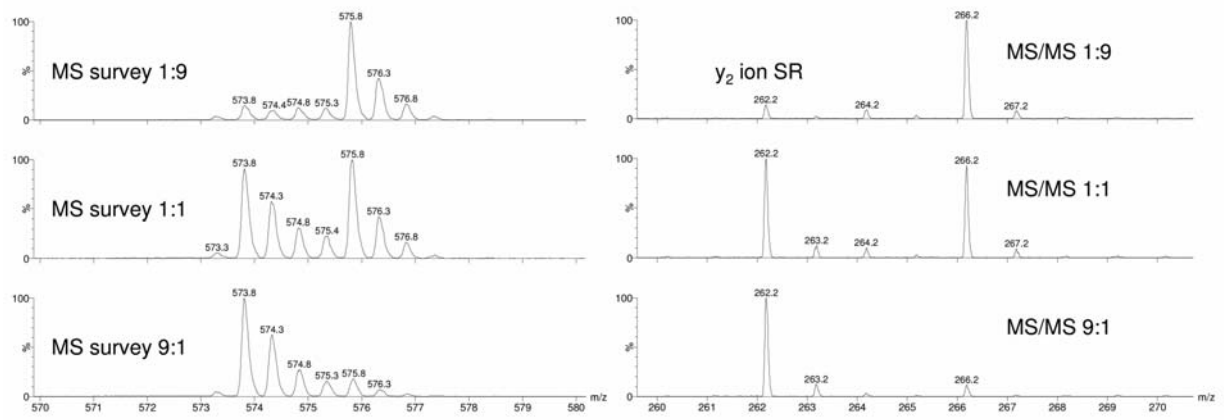

Figure 2. *Survey spectra (left panels) showing the intact precursor ions, and MS/MS spectra (right panels) showing the y_2 ions of a 1:9, 1:1 and 9:1 mixture of DLESQLAQSR ($C^{16}O^{16}OH$) and DLESQLAQSR ($C^{18}O^{18}OH$). The data were recorded by nanoESI-MS and -MS/MS, respectively. The related molecular and fragment ion patterns exhibit identical ratios between labeled and unlabeled species.*

fragment ions provide identical quantitative information. For the peptide mixtures investigated, all y ions from y_2 to y_7 can be used for quantification, whereas some deviations were observed for the y_1 and y_8 (=y_{max-2}) ions (see Supplementary Material, Figures S1 to S3). We feel that the somewhat variable ^{18}O content of these ions from the peptide ends might indicate a partial oxygen exchange during their formation. Exclusion of the corresponding data (y_1 ion and y_{max-2} ion) from the quantitative evaluation will therefore improve the accuracy of the quantitative data. However, this point was not followed in more detail in this study.

For relative quantification, there are several advantages of the MS/MS mode compared to the MS mode: i) the isotopic overlap is reduced, in particular for small y ions; ii) MS/MS spectra exhibit in general a better signal to noise ratio due to the strongly reduced background (39); iii) the quantitative results can be based on a set of y ion patterns, allowing the recognition and exclusion of interferences; iv) the MS/MS mode by principle is less prone to interferences due to its increased specificity.

For the particular application of a QTOF instrument with its limited dynamic range, the MS/MS mode also provides a somewhat extended linear dynamic range for high precursor ion signals. Using the 1:1 mixture of DLESQLAQSR ($C^{16}O^{16}OH$) and DLESQLAQSR ($C^{18}O^{18}OH$), different sample concentrations (50 fmol/μl to 50 pmol/μl), representing a dynamic range of 3 orders of magnitude, were quantified by nanoESI-MS and -MS/MS, respectively. Using quantification from the MS/MS spectra, a correct quantification over the whole range of concentrations with a maximal error of about 10% was possible. Quantification *via* the MS survey spectra resulted in a smaller dynamic range of only one order of magnitude (see Supplementary Material, Figure S4).

Relative quantification of standard protein mixtures by $^{16}O/^{18}O$ labeling. For evaluation of the complete workflow consisting of an automated UPLC-MS/MS analysis and subsequent quantitative data evaluation using MASCOT 2.2, a set of ovalbumin digest mixtures was prepared. Equal amounts of ovalbumin were digested in solution in either ^{16}O or ^{18}O water as described in Material and Methods. Measured aliquots of these samples were then mixed so that a set of samples with known ratios of ^{16}O to ^{18}O between 1:9 and 9:1 was obtained. These samples were analyzed by UPLC-MS/MS and the data files were transformed to peak lists and subsequently quantified using MASCOT 2.2 *via* its implemented ^{18}O quantification tool. All y ions with a possible interference by other sequence ions were automatically excluded from quantification. The minimal number of y ions required for quantification was 4 and the intensity cut-off was 0.1 (all ions with a relative abundance <10% were excluded from quantification). Using these settings, 26 tryptic ovalbumin peptides were identified on average in a single experiment, of which an average of 23 fulfilled the criteria for inclusion in the quantification. All experiments were carried out in triplicate and the quantitative data are summarized in Figure 3 (with the standard deviation (S.D.) and correlation coefficient (R^2)).

For all $^{16}O/^{18}O$ mixtures of ovalbumin peptides analyzed, very good agreement between the theoretical and experimental ratios, as indicated by the good R^2 value for the linear regression of the data set, was achieved, as shown in Figure 3. The small S.D. values demonstrate the good reproducibility of the method. This indicates successful optimization of the instrumental parameters for data acquisition, reproducible data acquisition by the UPLC-MS/MS system and correct selection of the parameters used for the automated evaluation by MASCOT.

$^{16}O/^{18}O$ Labeling and MS/MS analysis in a quantitative proteomic study. To evaluate the combination of $^{16}O/^{18}O$ labeling and MS/MS-based relative quantification for proteomic studies, we used this strategy to analyze the dynamics of the phosphoproteome in mouse cerebellum following treatment with ionizing radiation. Ten-day-old mice were treated with 10 Gy of ionizing radiation, and 1 h later cerebella were excised and proteins were extracted and digested by trypsin in either ^{18}O or ^{16}O water. Peptides were subsequently fractionated by SCX/WAX chromatography and IMAC as described in Materials and Methods. The resulting peptide and phosphopeptide fractions were then analyzed individually by UPLC-MS/MS using the methods described above. The MS/MS spectra of the individual fractions were transformed into peak list files and then merged into a single file. This file was searched against the MSDB database by MASCOT 2.2, which resulted in the simultaneous identification and quantification of a large set of peptides and phosphopeptides. In total, 342 proteins were quantified with an average ratio of 0.9 of irradiated to control sample. An overview of the results obtained for protein quantification is shown in Figure 4, and a detailed list of all proteins quantified is provided by Table S1 in the supplementary material.

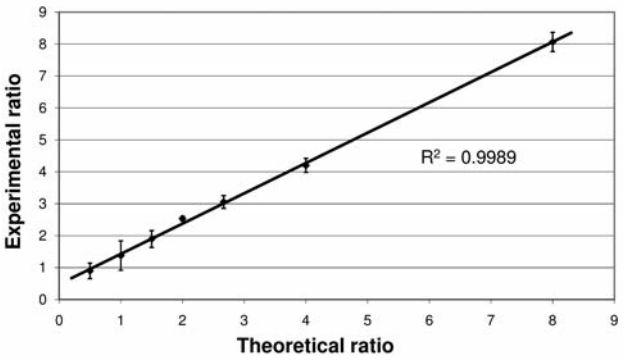

Figure 3. *Comparison of theoretical and experimental ratios for different mixtures of tryptic ovalbumin digests prepared in $H_2{}^{16}O$ or $H_2{}^{18}O$. After digestion, samples were mixed in the ratios indicated, analyzed by UPLC-MS/MS, and quantified by MASCOT 2.2. The data points are arithmetic means±1 S.D. (n=3).*

Discussion

The data in Figure 4 imply that the ratios of 8 proteins (irradiated over control) were outside the ±3 S.D. values set as cut-off. Manual examination indicated that 4 of these proteins contained regulated phosphopeptides which were taken for quantification as well, which means that the amount of these protein was probably not regulated. The remaining 4 proteins were: hemoglobin beta major chain (Figure 4, spot #1), heat-shock protein 70 (Hsp70) (#2), Ran-specific GTPase-activating protein (RANBP1) (#5) and protein kinase C and casein kinase substrate in neurons protein 1 (PACSIN1) (#6). Due to the role of hemoglobin as major constituent of red blood cells (41), the up-regulation may indicate increased perfusion of the cerebellum following irradiation. The early up-regulation of Hsp70 (1 h) after various types of stress including DNA damage has been reported (42, 43). RANBP1 regulates the activity of the GTPase Ran, which is responsible for the transport of molecules from the nucleus to the cytoplasm, including transport of p53 which plays a crucial role in apoptosis, one of the possible reactions of cells to DNA-damage (44-46). The role of PACSIN1 in the DNA damage response is currently unclear.

To further investigate the DNA damage response at the level of posttranslational modifications, phosphorylation site analysis was performed. In total, 174 phosphopeptides were identified and simultaneously quantified. The summarized phosphopeptide data are shown in Figure 5 and a list of all phosphopeptides is presented in Table S2 in the supplementary material.

As implied by the data shown in Figure 5, the majority of the identified phosphopeptides (86%) are not regulated, while 14% of the phosphopeptides showed more than 2-fold alteration of their ratio (irradiated sample over control) between the two samples. Based on these criteria, 24 phosphorylation sites altered in their concentration were identified. The proteins carrying these sites, their sequence coverage, phosphorylation sites identified, and the extent of their regulation are summarized in Table I. For regulated phosphorylation sites, the sequence motifs ±10 residues relative to the phosphorylated residue (see Table S3) were matched to known kinase consensus sequences. Seventeen of them could be potential targets of one of the following protein kinases: protein kinase B (Akt) ([RK]X[RK]XX[ST] (47)), cAMP-dependent protein kinase (PKA) (R[X]1-2-[ST] (48, 49)), casein kinase II (CK2) ([ST]AAAAA (48)), mitogen-activated protein kinase kinase (MAPKK)/extracellular signal-regulated kinase 2 (ERK2) (both PX[S/T]P (48)), and cyclin-dependent kinase 5 (Cdk5) (X[S/T]PXK (50)) where X is any residue, A is an acidic residue and [S/T] is the phosphorylated serine/threonine residue.

The up-regulation of ERK2 phosphorylation indicates activation of the ERK1/2 MAP kinase cascade, which has been associated with DNA damage (66). ERK signalling has been specifically associated with apoptotic response to DNA damage (67). One of the substrates identified for ERK2 in that study was RRAS2 (68). RRAS2 is a Ras homolog, however, in contrast to Ras, it does not activate the ERK pathway but rather the c-Jun *N*-terminal kinase (JNK) and p38 MAPK pathways (69). This links ERK signalling, which is known to be activated by extracellular signals such as growth factors, to p38 and JNK signalling which is stress-related, combining 3 of the major MAPK signalling pathways (70). Phosphorylation of the other two substrates

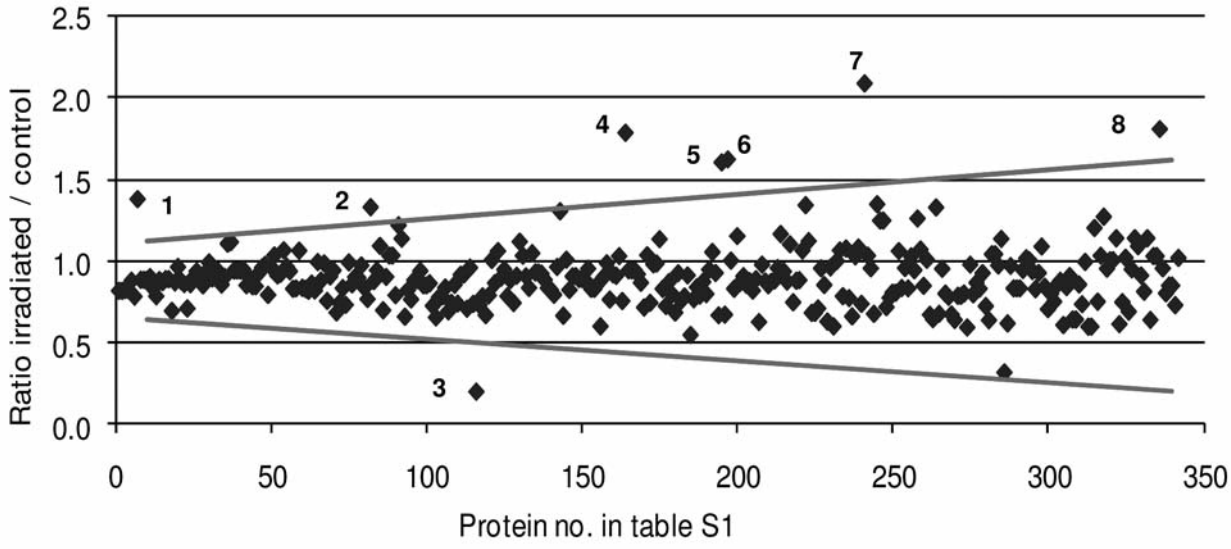

Figure 4. *Relative quantification of proteins from mouse brain cell lysates. The ratio data (irradiated over control) of 10 proteins were summarized successively and their arithmetic mean and S.D. were calculated. The red lines indicate the ±3 S.D. limits of the arithmetic means calculated in this way.*

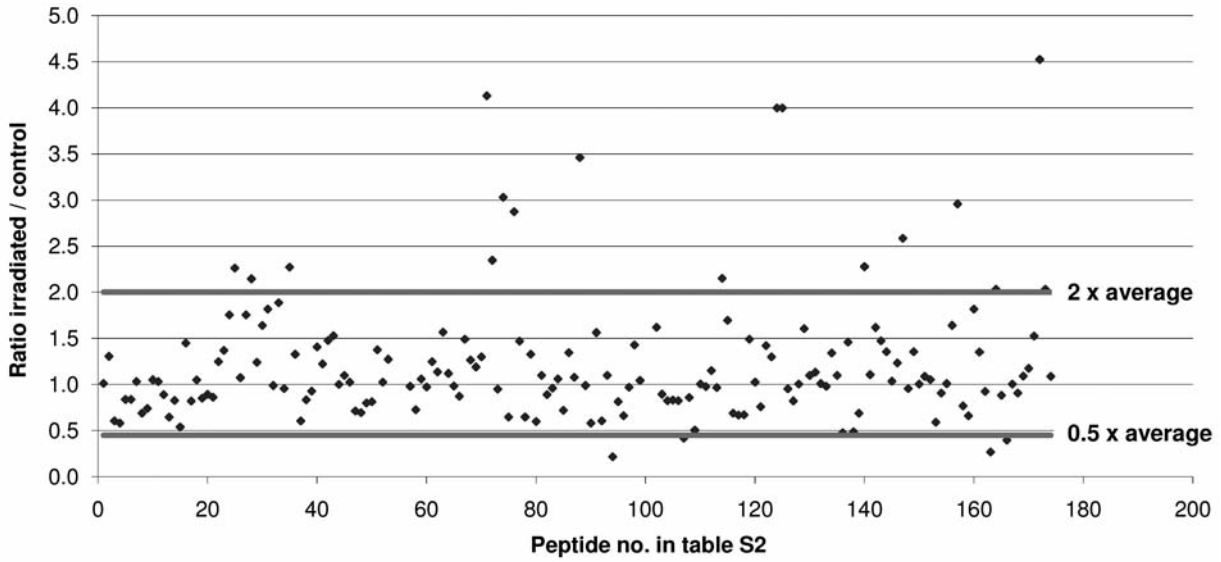

Figure 5. *MS/MS-based $^{16}O/^{18}O$ quantification of phosphopeptides identified in the analysis of the mouse brain cell lysates. As cut-off value indicating a regulated phosphopeptide, a two fold up- or down-regulation of the ratio observed in the protein quantification data was selected.*

of ERK2, MARCKS and MAP1A was found to be down-regulated. This may result from further modification of these proteins upon ERK phosphorylation.

The identification of 3 up-regulated Cdk5 substrates indicates an elevated activity of this kinase as well. Cdk5 is activated by ERK1/2 (71) and interleukin 6 (IL-6), the secretion of which is initiated by thymosin 4-beta (72, 73). A thymosin 4-beta phosphorylation site was found to be up-regulated, which may result in enhanced IL-6 secretion. The activation of Cdk5 following DNA damage has been shown to result in phosphorylation of Huntingtin regulating its toxicity in neurons (74). Cdk5 also phosphorylates p53, regulating its activity and inducing neuronal cell death (75). The targets of Cdk5, which carry regulated phosphorylation sites in this study, have not yet been associated with DNA damage. Three proteins containing up-regulated phosphorylation sites (Crmp2, Map2, Mapt) are microtubule-associated proteins. Map2 and Mapt are responsible for microtubule stabilization

Table I. *Proteins identified in mouse cerebellum containing phosphorylation sites regulated within 1 hour after irradiation. The ratio of irradiated vs. non-irradiated is indicated, as well as the matching to consensus targets of known protein kinases (?=no match).*

Protein	Sequence coverage (%)	Identified phosphorylation sites	Regulated phosphorylation sites	Target-kinase	Ratio	Function
ERK2	31	T183, Y185	T183, Y185	MAPKK	4.5	Member of MAP kinase pathway(51)
TRAP150	39	S248, S679	S679	?	2.3	Transcriptional coactivator(52)
SAFB2	23	S411	S411	?	0.4	Substrate of ATR or ATM(53)
MARCKS	47	S113, S138, S151	S113	ERK2	0.3	Substrate of PKC(54)
Bckdha	17	S334	S334	?	1.8	Branched chain ketoacid dehydrogenase
RRAS2	12	S186	S186	ERK2	2.0	Ras-related GTPase(55)
Doublecortin	45	S115, S305, S329, S339, S342	S305	PKA	3.0	Microtubuli-associated protein, substrate of Cdk5 and PKA
R3hdm2	15	S380, T294	S380	?	2.6	Binding of single-stranded DNA (56)
Dnajc5	14	S10	S10	Akt	0.5	Substrate of Akt
Thymosin beta-4	100	S2	S2	?	2.2	Forms 1:1 complex with G-actin (57)
P140CAP	31	S579, S1054, S1110	S579	PKA	4.0	Cytoskeleton regulator (58)
			S1110	CK2	4.0	
MAP1A	29	S548, S858, S1125, S1284, S1287, S1298, S1442, S2256	S548	ERK2	0.5	Microtubule-associated protein (59)
Reticulon1	10	S352	S352	CK2	0.5	Localized at ER, multiple functions in trafficking and apoptosis (60)
Rims1	32	S962	S962	PKA	2.3	Localized at synapses (61)
Crmp2	63	T509, S514, S522	T509	?	2.2 1.8	Differentiation of neuronal cells (62)
			S514, S522	?, Cdk5		
Map2	39	S894, S1013, S1160, S1783	S1013	PKA/Cdk5	2.3	Microtubule-associated, involved in axon development (63)
Mapt	59	S129, S130, S130, S133, S327, S331, S335, S345, S348	S331	?	2.4	Microtubule-associated, similar functions as Map2 (64)
			S335	Cdk5	4.1	
			S348	?	3.0	
MRP	44	S22	S22	Cdk5	0.2	MARCKS homolog (65)

(63), and Crmp2 is member of the Unc-33-like phospho-(Ulip) protein family whose members are associated with development and differentiation of neurons (62). The association of Cdk5 with microtubules and Cdk5-dependent phosphorylation of microtubule-associated proteins has been shown before and it was postulated that this may regulate the axonal transport of molecules in the cell (76). The activation of Cdk5 upon DNA damage may therefore be due to a elevated level of protein transport in the cell, either to start repair processes of the damaged DNA or to initiate apoptosis.

Another kinase found to be involved in signalling upon DNA damage is PKA. PKA has already been associated with DNA damage checkpoint pathways (77). It was also shown, that Cdk5 and PKA phosphorylate similar proteins while phosphorylation of a particular site by PKA influences phosphorylation of the same proteins by Cdk5 on another site (78). Two phosphorylation sites (on MAP2 and Crmp2) resemble the consensus sequence of both Cdk5 and PKA. These proteins may be phosphorylated by both kinases resulting in a crosstalk between their signalling pathways. Three other phosphorylation sites were identified to be PKA-dependent. One of them is S305 in Doublecortin, a microtubule-associated protein. Doublecortin, involved in the leading processes of migrating neurons, is a known target of PKA (S47) and Cdk5 (S297). These phosphorylations result in reduced affinity to microtubules (79, 80). The second site is located at P140CAP, which is involved in epidermal growth factor (EGF) and integrin signalling, which plays a role in actin cytoskeleton organisation and regulates Csk and Src kinase activity (58, 81). The third site was found in Rims1, which is a protein of the active zone of neurotransmitter release at synapses (61). It was shown that PKA activates the ERK signalling pathway *via* Ras/B-Raf and the p38 pathway *via* PTPs (70). Activation of ERK and p38MAPK again results in activation of the stress response of the cell.

CK2 is a constitutively active kinase with hundreds of known targets (82). For instance, it phosphorylates the checkpoint kinase Rad53 upon DNA damage and phosphorylation of MDC1 by CK2 is essential for proper accumulation of damage-response proteins at DNA double-strand breaks (83-85). CK2 is stabilized by interaction with ATR after DNA damage and phosphorylates the phosphatase and tensin homolog (PTEN) which is involved in cell cycle re-entry following DNA damage (86). Cell cycle re-entry of post-mitotic cells (*e.g.* neuronal cells) was reported to be involved in DNA damage-induced apoptosis (46).

Phosphorylation of Dnajc5 by Akt was shown *in vitro* and was linked to the late stages of exocytosis (87). The phosphorylation and activation of Akt following DNA damage was shown as well (88). In another study, Akt activation was linked to phosporylation by DNA-PK upon DNA damage, which resulted in stabilization of p53 by Akt (89). Interestingly, in this study, the phosphorylation of Dnajc5 was down-regulated by irradiation. This may be due to activation of a phosphatase, additional unexpected modifications of this region of Dnajc5 or degradation following phosphorylation.

Conclusion

Quantification of proteolytic ^{18}O-labeled peptides using MS/MS information is a powerful and easy tool for the quantification of proteins. By the use of MASCOT 2.2, quantification is convenient and platform independent, which allows the use of different types of mass spectrometers without the need of data transformation or the use of algorithms that suit different data formats. Using a QTOF instrument in the MS/MS mede, the linear range of the applicable sample amount is superior compared to survey-based quantification. Identification and quantification are carried out simultaneously. Using this technology, a detailed insight into the regulation of protein levels and phosphorylation sites can be conveniently achieved.

Acknowledgements

This work was supported by the Cooperation Program in Cancer Research of the German Cancer Research Center (DKFZ) and the Israeli Ministry of Science and Technology (MOST).

References

1 Schnolzer M, Jedrzejewski P and Lehmann WD: Protease-catalyzed incorporation of O-18 into peptide fragments and its application for protein sequencing by electrospray and matrix-assisted laser desorption/ionization mass spectrometry. Electrophoresis *17*: 945-953, 1996.

2 Mo WJ, Takao T and Shimonishi Y: Accurate peptide sequencing by post-source decay matrix-assisted laser desorption/ionization time-of-flight mass spectrometry. Rapid Commun Mass Spectrom *11*: 1829-1834, 1997.

3 Shevchenko A, Chernushevich I, Ens W, Standing KG, Thomson B, Wilm M and Mann M: Rapid '*de novo*' peptide sequencing by a combination of nanoelectrospray, isotopic labeling and a quadrupole/time-of-flight mass spectrometer. Rapid Commun Mass Spectrom *11*: 1015-1024, 1997.

4 Uttenweiler-Joseph S, Neubauer G, Christoforidis A, Zerial M and Wilm M: Automated *de novo* sequencing of proteins using the differential scanning technique. Proteomics *1*: 668-682, 2001.

5 Mirgorodskaya OA, Kozmin YP, Titov MI, Korner R, Sonksen CP and Roepstorff P: Quantitation of peptides and proteins by matrix-assisted laser desorption/ionization mass spectrometry using O-18-labeled internal standards. Rapid Commun Mass Spectrom *14*: 1226-1232, 2000.

6 Sakai J, Kojima S, Yanagi K and Kanaoka M: O-18-labeling quantitative proteomics using an ion-trap mass spectrometer. Proteomics *5*: 16-23, 2005.

7 Blonder J, Yu LR, Radeva G, Chan KC, Lucas DA, Waybright TJ, Issaq HJ, Sharom FJ and Veenstra TD: Combined chemical and enzymatic stable isotope labeling for quantitative profiling of detergent-insoluble membrane proteins isolated using Triton X-100 and Brij-96. J Proteome Res *5*: 349-360, 2006.

8 Hood BL, Lucas DA, Kim G, Chan KC, Blonder J, Issaq HJ, Veenstra TD, Conrads TP, Pollet I and Karsan A: Quantitative analysis of the low molecular weight serum proteome using O-18 stable isotope labeling in a lung tumor xenograft mouse model. J Am Soc Mass Spectrom *16*: 1221-1230, 2005.

9 Qian WJ, Monroe ME, Liu T, Jacobs JM, Anderson GA, Shen YF, Moore RJ, Anderson DJ, Zhang R, Calvano SE, Lowry SF, Xiao WZ, Moldawer LL, Davis RW, Tompkins RG, Camp DG and Smith RD: Quantitative proteome analysis of human plasma following *in vivo* lipopolysaccharide administration using O-16/O-18 labeling and the accurate mass and time tag approach. Mol Cell Proteomics *4*: 700-709, 2005.

10 Staes A, Demol H, Van Damme J, Martens L, Vandekerckhove J and Gevaert K: Global differential non-gel proteomics by quantitative and stable labeling of tryptic peptides with oxygen-18. J Proteome Res *3*: 786-791, 2004.

11 Yao XD, Freas A, Ramirez J, Demirev PA and Fenselau C: Proteolytic O-18 labeling for comparative proteomics: Model studies with two serotypes of adenovirus. Anal Chem *73*: 2836-2842, 2001.

12 Zang L, Toy DP, Hancock WS, Sgroi DC and Karger BL: Proteomic analysis of ductal carcinoma of the breast using laser capture microdissection, LC-MS, and O-16/O-18 isotopic labeling. J Proteome Res *3*: 604-612, 2004.

13 Bonenfant D, Schmelzle T, Jacinto E, Crespo JL, Mini T, Hall MN and Jenoe P: Quantitation of changes in protein phosphorylation: A simple method based on stable isotope labeling and mass spectrometry. Proc Natl Acad Sci USA *100*: 880-885, 2003.

14 Gonzalez J, Takao T, Hori H, Besada V, Rodriguez R, Padron G and Shimonishi Y: A method for determination of N-glycosylation sites in glycoproteins by collision-induced dissociation analysis in fast-atom-bombardment mass-spectrometry - identification of the positions of carbohydrate-linked asparagine in recombinant alpha-amylase by treatment with peptide-N-glycosidase-F in O-18-labeled water. Anal Biochem *205*: 151-158, 1992.

15 Kuster B and Mann M: O-18-Labeling of *N*-glycosylation sites to improve the identification of gel-separated glycoproteins using peptide mass mapping and database searching. Anal Chem *71*: 1431-1440, 1999.

16 Reynolds KJ, Yao XD and Fenselau C: Proteolytic O-18 labeling for comparative proteomics: Evaluation of endoprotease Glu-C as the catalytic agent. J Proteome Res *1*: 27-33, 2002.

17 Lindquist JA and McFadden PN: Incorporation of 2 O-18 atoms into a peptide during isoaspartyl repair reveals repeated passage through a succinimide intermediate. J Protein Chem *13*: 553-560, 1994.

18 Schindler P, Muller D, Marki W, Grossenbacher H and Richter WJ: Characterization of a beta-Asp33 isoform of recombinant hirudin sequence variant 1 by low-energy collision-induced dissociation. J Mass Spectrom *31*: 967-974, 1996.

19 Xiao G, Bondarenko PV, Jacob J, Chu GC and Chelius D: O-18 labeling method for identification and quantification of succinimide in proteins. Anal Chem *79*: 2714-2721, 2007.
20 Li XJ, Cournoyer JJ, Lin C and O'Cormora PB: Use of O-18 labels to monitor deamidation during protein and peptide sample processing. J Am Soc Mass Spectrom *19*: 855-864, 2008.
21 Miyagi M and Rao KCS: Proteolytic O-18-labeling strategies for quantitative proteomics. Mass Spectrom Rev *26*: 121-136, 2007.
22 Stewart, II, Thomson T and Figeys D: O-18 Labeling: a tool for proteomics. Rapid Commun Mass Spectrom *15*: 2456-2465, 2001.
23 Bantscheff M, Schirle M, Sweetman G, Rick J and Kuster B: Quantitative mass spectrometry in proteomics: a critical review. Anal Bioanal Chem *389*: 1017-1031, 2007.
24 Fenselau C: A review of quantitative methods for proteomic studies. J Chrom B Anal Tech Biomed Life Sci *855*: 14-20, 2007.
25 Heck AJR and Krijgsveld J: Mass spectrometry-based quantitative proteomics. Exp Rev Proteomics *1*: 317-326, 2004.
26 Mann M: Functional and quantitative proteomics using SILAC. Nat Rev Mol Cell Biol *7*: 952-958, 2006.
27 Mayya V and Han DK: Proteomic applications of protein quantification by isotope-dilution mass spectrometry. Exp Rev Proteomics *3*: 597-610, 2006.
28 Mirza SP, Greene AS and Olivier M: O-18 Labeling over a coffee break: A rapid strategy for quantitative proteomics. J Proteome Res *7*: 3042-3048, 2008.
29 Carreira RJ, Rial-Otero R, Lopez-Ferrer D, Lodeiro C and Capelo JL: Ultrasonic energy as a new tool for fast isotopic O-18 labeling of proteins for mass spectrometry-based techniques: Preliminary results. Talanta *76*: 400-406, 2008.
30 Rao KCS, Palamalai V, Dunlevy JR and Miyagi M: Peptidyl-Lys metalloendopeptidase-catalyzed O-18 labeling for comparative proteomics–Application to cytokine/lipolysaccharide-treated human retinal pigment epithelium cell line. Mol Cell Proteomics *4*: 1550-1557, 2005.
31 Hajkova D, Rao KCS and Miyagi M: pH dependency of the carboxyl oxygen exchange reaction catalyzed by lysyl endopeptidase and trypsin. J Proteome Res *5*: 1667-1673, 2006.
32 Angel PM, Lim JM, Wells L, Bergmann C and Orlando R: A potential pitfall in O-18-based *N*-linked glycosylation site mapping. Rapid Commun Mass Spectrom *21*: 674-682, 2007.
33 Angel PM and Orlando R: Trypsin is the primary mechanism by which the O-18 isotopic label is lost in quantitative proteomic studies. Anal Biochem *359*: 26-34, 2006.
34 Storms HF, van der Heijden R, Tjaden UR and van der Greef J: Considerations for proteolytic labeling-optimization of O-18 incorporation and prohibition of back-exchange. Rapid Commun Mass Spectrom *20*: 3491-3497, 2006.
35 Sevinsky JR, Brown KJ, Cargile BJ, Bundy JL and Stephenson JL: Minimizing back exchange in O-18/O-16 quantitative proteomics experiments by incorporation of immobilized trypsin into the initial digestion step. Anal Chem *79*: 2158-2162, 2007.
36 Johnson KL and Muddiman DC: A method for calculating O-16/O-18 peptide ion ratios for the relative quantification of proteomes. J Am Soc Mass Spectrom *15*: 437-445, 2004.
37 Hicks WA, Halligan BD, Slyper RY, Twigger SN, Greene AS and Olivier M: Simultaneous quantification and identification using O-18 labeling with an ion trap mass spectrometer and the analysis software application "ZoomQuant". J Am Soc Mass Spectrom *16*: 916-925, 2005.
38 Mason CJ, Therneau TM, Eckel-Passow JE, Johnson KL, Oberg AL, Olson JE, Nair KS, Muddiman DC and Bergen HR: A method for automatically interpreting mass spectra of 180-labeled isotopic clusters. Mol Cell Proteomics *6*: 305-318, 2007.
39 Zhang GA and Neubert TA: Automated comparative proteomics based on multiplex tandem mass spectrometry and stable isotope labeling. Mol Cell Proteomics *5*: 401-411, 2006.
40 Winter D, Seidler J, Ziv Y, Shiloh Y and Lehmann WD: Citrate boosts the performance of phosphopeptide analysis by UPLC-ESI-MS/MS. J Proteome Res *8*: 418-424, 2009.
41 Goodman SR, Kurdia A, Ammann L, Kakhniashvili D and Daescu O: The human red blood cell proteome and interactome. Experimental Biol Med *232*: 1391-1408, 2007.
42 Sanchez-Rodriguez SH, Lopez-Luna A, Avalos-Diaz E and Herrera-Esparza R: Cell stress induces association of heat-shock proteins with the cytoskeleton. J Biol Res Thessaloniki *9*: 67-74, 2008.
43 Valbonesi P, Franzellitti S, Piano A, Contin A, Biondi C and Fabbri E: Evaluation of HSP70 expression and DNA damage in cells of a human trophoblast cell line exposed to 1.8 GHz amplitude-modulated radiofrequency fields. Radiation Res *169*: 270-279, 2008.
44 Ciciarello M, Mangiacasale R and Lavia P: Spatial control of mitosis by the GTPase Ran. Cell Mol Life Sci *64*: 1891-1914, 2007.
45 Clarke PR and Zhang CM: Spatial and temporal coordination of mitosis by Ran GTPase. Nat Rev Mol Cell Biol *9*: 464-477, 2008.
46 Barzilai A, Biton S and Shiloh Y: The role of the DNA damage response in neuronal development, organization and maintenance. DNA Repair *7*: 1010-1027, 2008.
47 Ballif BA, Villen J, Beausoleil SA, Schwartz D and Gygi SP: Phosphoproteomic analysis of the developing mouse brain. Mol Cell Proteomics *3*: 1093-1101, 2004.
48 Aitken A: Protein consensus sequence motifs. Mol Biotech *12*: 241-253, 1999.
49 Seidler J, Adal M, Kübler D, Bossemeyer D and Lehmann WD: Analysis of autophosphorylation sites in the recombinant catalytic subunit alpha of cAMP-dependent kinase by nanoUPLC-ESI-MS/MS. Anal Bioanal Chem *395*: 1713-1720, 2009.
50 Kesavapany S, Li BS and Pant HC: Cyclin-dependent kinase 5 in neurofilament function and regulation. Neurosignals *12*: 252-264, 2003.
51 Sturgill TW: MAP kinase: It's been longer than fifteen minutes. Biochem Biophys Res Commun *371*: 1-4, 2008.
52 Ito M, Yuan CX, Malik S, Gu W, Fondell JD, Yamamura S, Fu ZY, Zhang XL, Qin J and Roeder RG: Identity between TRAP and SMCC complexes indicates novel pathways for the function of nuclear receptors and diverse mammalian activators. Mol Cell *3*: 361-370, 1999.
53 Matsuoka S, Ballif BA, Smogorzewska A, McDonald ER, Hurov KE, Luo J, Bakalarski CE, Zhao ZM, Solimini N, Lerenthal Y, Shiloh Y, Gygi SP and Elledge SJ: ATM and ATR substrate analysis reveals extensive protein networks responsive to DNA damage. Science *316*: 1160-1166, 2007.
54 Herget T, Oehrlein SA, Pappin DJC, Rozengurt E and Parker PJ: The myristoylated alanine-rich C-kinase substrate (Marcks) is sequentially phosphorylated by conventional, novel and atypical isotypes of protein-kinase-C. Eur Journal Biochem *233*: 448-457, 1995.
55 Bos JL: Ras-like GTPases. Biochim Biophys Acta Rev Cancer *1333*: M19-M31, 1997.
56 Grishin NV: The R3H motif: A domain that binds single-stranded nucleic acids. Trends Biochem Sci 23: 329-330, 1998.

57 Safer D and Nachmias VT: Beta-thymosins as actin-binding peptides. Bioessays *16*: 473-479, 1994.
58 Di Stefano P, Cabodi S, Erba EB, Margaria V, Bergatto E, Giuffrida MG, Silengo L, Tarone G, Turco E and Defilippi P: p130Cas-associated protein (p140Cap) as a new tyrosine-phosphorylated protein involved in cell spreading. Mol Biol Cell *15*: 787-800, 2004.
59 Halpain S and Dehmelt L: The MAPI family of microtubule-associated proteins. Genome Biol *7*: 224-, 2006.
60 Iwahashi J, Hamada N and Watanabe H: Two hydrophobic segments of the RTN1 family determine the ER localization and retention. Biochem Biophys Res Commun *355*: 508-512, 2007.
61 Schoch S, Castillo PE, Jo T, Mukherjee K, Geppert M, Wang Y, Schmitz F, Malenka RC and Sudhof TC: RIM1 alpha forms a protein scaffold for regulating neurotransmitter release at the active zone. Nature *415*: 321-326, 2002.
62 Byk T, Ozon S and Sobel A: The Ulip family phosphoproteins–Common and specific properties. Eur J Biochem *254*: 14-24, 1998.
63 Al-Bassam J, Ozer RS, Safer D, Halpain S and Milligan RA: MAP2 and tau bind longitudinally along the outer ridges of microtubule protofilaments. J Cell Biol *157*: 1187-1196, 2002.
64 Couchie D, Gache Y, Mavilia C, Guilleminot J, Bridoux AM, Nivez MP and Nunez J: High-molecular-weight tau proteins and acquisition of neuronal polarity in the peripheral nervous-system. Comptes Rendus De L Academie Des Sciences Serie Iii-Sciences De La Vie-Life Sciences *316*: 404-409, 1993.
65 Li JX and Aderem A: Macmarcks, a novel member of the marcks family of protein-kinase-C substrates. Cell *70*: 791-801, 1992.
66 Dent P, Yacoub A, Fisher PB, Hagan MP and Grant S: MAPK pathways in radiation responses. Oncogene *22*: 5885-5896, 2003.
67 Tang DM, Wu DH, Hirao AH, Lahti JM, Liu LQ, Mazza B, Kidd VJ, Mak TW and Ingram AJ: ERK activation mediates cell cycle arrest and apoptosis after DNA damage independently of p53. J Biol Chem *277*: 12710-12717, 2002.
68 Olsen JV, Blagoev B, Gnad F, Macek B, Kumar C, Mortensen P and Mann M: Global, *in vivo*, and site-specific phosphorylation dynamics in signaling networks. Cell *127*: 635-648, 2006.
69 Graham SM, Oldham SM, Martin CB, Drugan JK, Zohn IE, Campbell S and Der CJ: TC21 and Ras share indistinguishable transforming and differentiating activities. Oncogene *18*: 2107-2116, 1999.
70 Gerits N, Kostenko S, Shiryaev A, Johannessen M and Moens U: Relations between the mitogen-activated protein kinase and the cAMP-dependent protein kinase pathways: Comradeship and hostility. Cell Signalling *20*: 1592-1607, 2008.
71 Lee JH and Kim KT: Regulation of cyclin-dependent kinase 5 and p53 by ERK1/2 pathway in the DNA damage-induced neuronal death. J Cell Physiol *210*: 784-797, 2007.
72 Zhang YQ, Feurino LW, Zhai QH, Wang H, Fisher WE, Chen CY, Yao QZ and Li M: Thymosin beta 4 is overexpressed in human pancreatic cancer cells and stimulates proinflammatory cytokine secretion and JNK activation. Cancer Biol Therapy *7*: 419-423, 2008.
73 Quintanilla RA, Orellana DI, Gonzalez-Billault C and Maccioni RB: Interleukin-6 induces Alzheimer-type phosphorylation of tau protein by deregulating the cdk5/p35 pathway. Exper Cell Res *295*: 245-257, 2004.
74 Anne SL, Saudou F and Humbert S: Phosphorylation of Huntingtin by cyclin-dependent kinase 5 is induced by DNA damage and regulates wild-type and mutant Huntingtin toxicity in neurons. J Neurosci *27*: 7318-7328, 2007.
75 Lee JH, Kim HS, Lee SJ and Kim KT: Stabilization and activation of p53 induced by Cdk5 contributes to neuronal cell death. J Cell Sci *120*: 2259-2271, 2007.
76 Smith DS and Tsai LH: Cdk5 behind the wheel: a role in trafficking and transport? Trends Cell Biol *12*: 28-36, 2002.
77 Searle JS, Schollaert KL, Wilkins BJ and Sanchez Y: The DNA damage checkpoint and PKA pathways converge on APC substrates and Cdc20 to regulate mitotic progression. Nature Cell Biol *6*: 138-145, 2004.
78 Liu F, Liang ZH, Shi JH, Yin DM, El-Akkad E, Grundke-Iqbal I, Iqbal K and Gong CX: PKA modulates GSK-3 beta- and cdk5-catalyzed phosphorylation of tau in site- and kinase-specific manners. FEBS LET *580*: 6269-6274, 2006.
79 Schaar BT, Kinoshita K and McConnell SK: Doublecortin microtubule affinity is regulated by a balance of kinase and phosphatase activity at the leading edge of migrating neurons. Neuron *41*: 203-213, 2004.
80 Tanaka T, Serneo FF, Tseng H-C, Kulkarni AB, Tsai L-H and Gleeson JG: Cdk5 phosphorylation of Doublecortin Ser297 regulates its effect on neuronal migration. Neuron *41*: 215-227, 2004.
81 Di Stefano P, Damiano L, Cabodi S, Aramu S, Tordella L, Praduroux A, Piva R, Cavallo F, Forni G, Silengo L, Tarone G, Turco E and Defilippi P: p140Cap protein suppresses tumour cell properties, regulating Csk and Src kinase activity. EMBO J *26*: 2843-2855, 2007.
82 Sarno S and Pinna LA: Protein kinase CK2 as a druggable target. Mol Biosys *4*: 889-894, 2008.
83 Guillemain G, Ma E, Mauger S, Miron S, Thai R, Guerois R, Ochsenbein F and Marsolier-Kergoat MC: Mechanisms of checkpoint kinase Rad53 inactivation after a double-strand break in Saccharomyces cerevisiae. Mol Cell Biology *27*: 3378-3389, 2007.
84 Spycher C, Miller ES, Townsend K, Pavic L, Morrice NA, Janscak P, Stewart GS and Stucki M: Constitutive phosphorylation of MDC1 physically links the MRE11-RAD50-NBS1 complex to damaged chromatin. J Cell Biol *181*: 227-240, 2008.
85 Wu LM, Luo KT, Lou ZK and Chen JJ: MDC1 regulates intra-S-phase checkpoint by targeting NBS1 to DNA double-strand breaks. Proc Natl Acad Sci USA *105*: 11200-11205, 2008.
86 Martin SA and Ouchi T: Cellular commitment to reentry into the cell cycle after stalled DNA is determined by site-specific phosphorylation of Chk1 and PTEN. Mol Cancer Therapeutics *7*: 2509-2516, 2008.
87 Evans GJ, Barclay JW, Prescott GR, Jo SR, Burgoyne RD, Birnbaum MJ and Morgan A: Protein kinase B/Akt is a novel cysteine string protein kinase that regulates exocytosis release kinetics and quantal size. J Biol Chem *281*: 1564-1572, 2006.
88 Viniegra JG, Martinez N, Modirassari P, Losa JH, Cobo CP, Lobo V, Luquero CIA, Alvarez-Vallina L, Cajal SRY, Rojas JM and Sanchez-Prieto R: Full activation of PKB/Akt in response to insulin or ionizing radiation is mediated through ATM. J Biol Chem *280*: 4029-4036, 2005.
89 Boehme KA, Kulikov R and Blattner C: P53 stabilization in response to DNA damage requires Akt/PKB and DNA-PK. Proc Natl Acad Sci USA *105*: 7785-7790, 2008.

Received June 2, 2009
Revised November 11, 2009
Accepted November 12, 2009